SHALLOW VELOCITY STRUCTURE AT THE SHAGAN RIVER TEST SITE IN KAZAKSTAN

Jessie L. Bonner, Southern Methodist University
D. Craig Pearson, W. Scott Phillips and Steven R. Taylor, Los Alamos National Laboratory

Sponsored by U.S. Department of Energy
Office of Non-Proliferation and National Security
Office of Research and Development
Contract No.: W-7405-ENG-36

ABSTRACT

During 1997 and 1998, 12 chemical explosions were detonated in boreholes at the former Soviet nuclear test site near the Shagan River in Kazakstan. These explosions were recorded at local distances by a network of seismometers operated by Los Alamos National Laboratory and the Institute of Geophysics for the National Nuclear Centre (NNC) in Kazakstan. The depths of these explosions ranged from 2.5 to 550 m, while the explosive yield varied from 2 to 25 tons.

Short-period, fundamental-mode Rayleigh waves (*Rg*) were generated by these explosions and recorded at the local stations, and the waves exhibited normal dispersion between 0.2 and 3 seconds. Dispersion curves were generated for each propagation path, and tomographic maps of *Rg* group velocity show a zone of fast velocities (> 2.3 km/sec for 1-second period *Rg*) for the southwestern section of the test site and slow propagation (≤ 2.3 km/sec) for the northeastern section. The two regions are separated by a thin NW-SE trending transitional zone that parallels the tectonic fabric for the study area. The group velocities correlate with spatial patterns of magnitude residuals (Ringdal and Marshall, 1989) from nuclear explosions at the Shagan River Test Site, and may help to evaluate the mechanisms behind those observations. The inversions of the *Rg* dispersion curves show shear wave velocities for the southwestern section that are on average 0.4 km/sec greater than the northeastern zone. At depths greater than 1.5 km, the standard deviations for the models begin to overlap, and the statistical difference between the models is no longer significant. The differences observed in the shear wave velocity structures above 1.5 km, for the various propagation paths, must be considered when making local to near-regional correlations of the explosions.

Key Words: *Rg* dispersion, shear wave velocity structure, Shagan River Test Site

OBJECTIVES

The properties of geological materials change quickly near the earth's surface. If these changes in geologic structure affect seismic generation from shallow (near-surface) and deep (up to 1-km) explosions differently, we may be able to develop techniques to discriminate between large industrial blasts and an underground nuclear test. For the present study, we attempt to determine the lateral variations in the velocity structure at the former Soviet test site near the Shagan River in Kazakhstan (STS) by using the properties of explosion generated *Rg*. *Rg* was observed on the local seismograms near the test site from a series of chemical explosions detonated at varying depths within the upper crust during 1997 and 1998. The purpose of the explosions was for the closure of the unused boreholes at the former test site as part of a joint project between the U.S. Department of Energy (DOE), the U.S. Defense Special Weapons Agency (DSWA), and the National Nuclear Center of the Republic of Kazakhstan (NNC). The explosions were recorded by a dense local network operated by Los Alamos National Laboratory and by a regional network operated by Lamont-Doherty Earth Observatory.

For explosions detonated on or near the earth's surface, *Rg* is often the dominant arrival at local to near-regional distances. *Rg* group velocities are controlled by the velocity variations in the upper few kilometers of crust along the propagation path. The phase is highly attenuated in regions of complex terrain, and is most prominent on paths comprised of low velocity sediments or weathered rock (Kocaoglu and Long, 1993). *Rg* is seldom recorded at distances greater than 300 km thus limiting its usefulness as a depth discriminant. However, the influence of *Rg* scattering into *Lg* coda from explosions has been noted and can make an important contribution to explosion seismograms [e.g. Gupta *et al*., 1992; Patton and Taylor, 1995; Mayeda and Walter, 1996; Meyer *et al.,* 1999].

Because *Rg* group velocities are controlled by the velocity variations in the upper few kilometers of crust, the surface geology of the path can offer insight into the characteristics of the propagation. The former test site has a complex structural and geologic setting created by the interaction of the Siberian and Kazakhstan continental plates and intervening island arcs (Zonenshain *et al.,* 1990). The region has undergone two periods of deformation as a result of the Caledonian and Hercynian orogenies. The Caledonian orogeny (early Paleozoic) is represented by varying degrees of faulting, folding, and metamorphism (Nalivkin, 1960). One of these faults, the Chinrau, dissects the former test site along a NW-SE trend and appears to show evidence of recent offset on SPOT imagery (Leith, 1987). It is the later Hercynian orogeny (Carboniferous) that folded the Carboniferous-aged sedimentary rocks and implaced the granites and granodiorites at the test site (Figure 1). The result of the compressive forces associated with these two orogenies is a NW-SE trending tectonic fabric. Quaternary sediments, including sands, clays, and gravel now cover a large portion of the test site. As can be inferred from Figure 1, the test site is not in a homogenous body of rock. In fact, the site can be divided into two regions--a northeastern (NE) region composed of alluvial and tuffaceous deposits overlying folded and faulted Paleozoic sedimentary rocks and a southwestern (SW) quadrant comprised of a large granodiorite body that intruded into the surrounding sedimentary rocks. This intrusive complex is encountered in boreholes 1327 and 1411, and can be inferred to connect beneath the alluvium. The lithology of this pluton has been referred to as granite and granodiorite (Davis and Berlin, 1992) and granodiorite (Borovikov, 1972). For the purpose of this paper, we refer to the pluton as crystalline rock. The results of this paper show how these variations in the shallow geology cause a large range of *Rg* group velocities.

RESEARCH ACCOMPLISHED

This study involves seismograms from 10 explosions at STS (Table 1). The explosions were conducted to seal the unused boreholes at the test site. The shots at boreholes 1071, 1311, 1349, and 1381 had an explosive weight of 25 tons and were emplaced at depths of 50 m, 50m, 300 m, and 550 m, respectively. At the intervals of the explosives emplacement, neogenic clays (1311) or crystalline rock (1071, 1349 and 1381) were observed. The primary scientific objective of this series of explosions was to determine the effect of depth of burial on the discrimination of nuclear explosions. A secondary objective was to calibrate the Kazakhstan seismic network, with special emphasis on the IRIS GSN station at Makanchi (MAK) and the IMS auxiliary stations Kurchatov (KUR) and Aktyubinsk (AKT). Results of the regional studies can be found in Glenn and Meyers (1997) and Meyers *et al*. (1999).

TABLE 1. EXPLOSION CHARACTERISTICS AT BOREHOLE CLOSURES

Borehole	Latitude	Longitude	Explosive weight (kg)	Depth of charge emplacement from surface (m)	Date	Origin Time (UTC)
1071	49.9810	78.7559	25000	28	9/17/98	07:19:40.551
1311	49.9412	78.7860	25000	50	8/3/97	08:07:20.039
1327	49.9129	78.7871	2028	20	7/14/98	05:11:35.570
1349	49.8794	78.8493	25000	550	08/5/97	07:30:15.126
1381	49.8837	78.8147	25000	300	8/31/97	07:08:39.179
1383	49.8724	78.6477	2028	14	8/15/98	02:40:59.116
1386	49.8801	78.6921	2028	20	7/13/98	10:44:56.363
1389	49.8786	78.7601	2028	9	08/15/98	05:05:11.156
1409	50.0357	79.0114	2028	13	8/14/98	04:28:52.815
1419	50.0576	78.9387	2028	2.5	08/14/98	05:39:24.970

In addition to the DOB study, 8 additional explosive borehole closures were recorded (Table 1). The depth of the explosives emplacement for these closures ranged from 2.5 to 46 meters with 2 ton yields. Boreholes 1071 and 1383 were detonated in granoseyenites, while the six other explosive closures in 1998 were conducted in neogenic clays.

A seismic network was deployed at local distances by Los Alamos National Laboratory to record the explosions, and the network was maintained for the duration of the program by the Institute of Geophysical Research (NNC). Seismograms were recorded on L4-C-3D, three-component, velocity sensors connected to Refraction Technology (REFTEK) data loggers. Origin times for each event were obtained by a GPS-based timing system employed at each hole for shot-break time. The origin times were checked for consistency using an accelerometer and data acquisition system placed near the test borehole. Seven sites were selected at various azimuths to the proposed locations for the DOB experiment (Table 2). For the 1998 series of hole closures, the seismic stations reoccupied the same DOB locales, except for S3 which was relocated because of technical problems. For the REFTEK/L4-C-3D sites, the data was sampled at 500 Hz, and the recorder was set up to use a STA/LTA trigger. The data was then transferred to a workstation at LANL for dispersion processing and analysis. The dispersion curves were generated through use of the Multiple Filter Analysis (Dziewonski *et al*., 1969) and refined by Phase Match Filtering (Herrin and Goforth, 1977).

TABLE 2. COORDINATES FOR THE BALAPAN NETWORK

Station	Latitude	Longitude
S2	49.8636	78.8701
S3[1]	49.8874	78.9087
S3	49.9494	78.7483
S4	49.8766	78.7636
S6	49.8217	78.7531
S7	49.8526	78.9841
S8	49.9777	78.7590
S9	49.9719	78.9587

The dispersion curves for all paths considered in this study are shown in Figure 2. Group velocities range from 1.7 up to 2.9 km/sec, and have periods between 0.2 and 3 seconds. A better way to show the same data is through the use of group velocity tomography maps for individual periods. Tomography was performed assuming straight ray propagation, parameterizing the model with an array of constant velocity circles. We used first-difference regularization to control the effects of noise on the final image.

[1] Location valid for Hole Closures 1311, 1349, and 1381

Regularization parameters were chosen to optimize resolution and covariance; further details may be found in Phillips *et al*. (1999). Tomographic inversion produced variance reduction of 80%, 94%, 78% and 66%, relative to a flat model, for periods of 0.5, 1.0, 1.5 and 2.0 seconds, respectively.

The group velocity tomography maps presented in Figures 3 – 5 show a relatively high velocity region to the southwest (SW), separated from a low velocity region in the northeast (NE) by a thin transition zone. We suspect that the faster velocities in the SW region are related to crystalline rocks at or near the surface. Logs for test hole 1383 (NNC Field Report, 1996) show crystalline rocks to within 5 m of the surface. At shorter periods of 0.5 and 1 sec (Figure 3 and Figure 4), the low velocities associated with the transition zone follow the Shagan River towards the southwest, and may be related to alluvium overlying the intrusive crystalline rocks near this section of the test site. Lithologic logs from boreholes in this region confirm that alluvium and weathered rock with thickness as great as 350 m overlie the crystalline rocks. For all period ranges, a region of low velocities is observed in the northeast. Lithologies for these boreholes include thick sections of alluvium and unconsolidated tuffs that overlie the Paleozoic sedimentary section.

We used least squares inversion technique (Herrmann, 1988) to invert group velocity dispersion curves for the shallow shear wave velocity structure within the different regions of the STS. Paths within each region of the test site were inverted using both differential and stochastic inversions for different starting velocity models. The minimum, maximum, and average shear wave velocity structures from all inversions for paths in the SW and transition regions of the test site are shown in Figure 6. The minimum velocity was obtained by inverting the paths that predominantly sample the rocks for the transition zone between the fast and slow regions (1327 and 1311 to S6, S7, and S4). The maximum velocity curve is the result of the path from shot 1383 to S3 and S8. These paths are confined in the granodiorite and have the greatest group velocities for the entire *Rg* bandwidth. The average velocity structure shows three distinct layers--a 250 m thick section with velocities averaging 2.45 km/sec, a layer between 250 m and 900 m with velocities averaging 2.95 km/sec, and a third layer to a depth of 2.5 km with shear wave velocities of approximately 3.3 km/sec.

Figure 7 shows the results of the inversions in the northeast region. The minimum velocity structure was obtained from the inversion of paths such as 1327 to S9 and 1311 to S9, both having flat, low-velocity dispersion curves. *Rg* along this path is slowed by propagation predominantly within the NE region. However, about 25% of the path occurs in the transition zone, thus creating a velocity structure with greater velocities than the average for the NE. Three distinct layers were noted in the velocity structure for the SW and transitional regions, while the suite of inversions in the NE region show the average velocity structure to be increasing with depth without prominent discontinuities down to a depth of approximately 2 km. Below this depth, the resolution is compromised, as *Rg* waves in this region have smaller wavelengths.

As discussed above, the trends from the tomographic inversion appear to delineate two distinct zones separated by a NW-SE trending boundary. Relatively high velocities are observed to the SW and lower velocities to the NE. The boundary separating the two zones roughly coincides with the Chinrau fault. Sequences of tuffs and alluvium exist to the northeast of this boundary overlying Paleozoic sedimentary rocks and to the southwest, crystalline rock is predominant. Differences between the NE and SW regions have been known for some time on the basis of teleseismic P-wave spectral and waveform differences from nuclear explosions (Marshall *et al*., 1984; Stewart, 1988; Bache *et al*., 1986). Additionally, more recent studies have indicated NE and SW contrasts in *Lg* amplitudes (Ringdal *et al*., 1992; Jih and Wagner, 1992). Specifically, Marshall *et al*., (1984) observed that *P* waves from Shagan Test Site (STS) nuclear explosions fell into two distinct classes. NE STS *P* waveforms are more complex and have higher corner frequencies than those from SW explosions of similar magnitude. The *P* waveforms from the NE explosions exhibit a few cycles of ringing not observed on the simple waveforms from the SW. This is consistent with the observed complexity of the NE *Rg* waves relative to those in the SW discussed earlier (Figs. 3 and 4). The observation of longer duration waveforms in the NE relative to SW STS conflicts with the spectral observations of Marshall *et al*. (1984). However, in comparing spectra for the two different regions at the UK array stations in Bache *et al*. (1986), the difference in the corner frequencies is not strongly apparent. It was suggested that changes in source material properties were the cause of the observed differences, although very little geologic information was available at the time. Stewart (1988) also noted the NE explosion *P* waveforms had a smaller, longer period, first negative pulse (presumably pP) than those from the SW. It was suggested that the greater P-pP times and longer period pP pulses were due to greater scaled depth of burial and/or slower uphole velocities in the northeast.

The spatial variations in velocities from this study (Figure 3-5 and Figures 6 and 7) are consistent with the observations of teleseismic *P* waves and *Lg* waves from STS nuclear explosions. For example, it is expected that explosions detonated in a region having low-velocity sedimentary layers overlying crystalline basement will show *P* waveforms that are more complex and lower frequency than those detonated in crystalline rock. The complex waveforms and larger pP delays are presumably due to near-surface reverberations and lower uphole velocities. The lower corner frequencies are predicted from established explosion-source models (e.g. Mueller and Murphy, 1971). Using a Mueller-Murphy explosion-source model for granite we compute Reduced Velocity Potential (RVP) spectra for two identical explosions. Each explosion had a yield of (150 kT) and near-source compressional velocities of 5 and 3.9 km/s taken from velocity models shown in Figures 6 and 7 (representing the SW and NE portions of the STS, respectively). The results are shown in Figure 8 and it can be seen that just based on simple elastic properties, we expect explosions of identical yields from the NE to have lower corner frequencies than those from the SW. The explosion-source corner frequency is proportional to the decay rate of the pressure-time history acting at the elastic radius, which in turn, is proportional to the compressional velocity at the source. Thus, the lower corner frequencies as evidenced by the longer duration *P* waves for the NE explosions may simply be due to the reduced velocities (e.g. material strength) in the near-source region.

CONCLUSIONS AND RECOMMENDATIONS

The results of this study show that variations in geologic structure have a significant effect on *Rg* group velocities at STS. Tomography maps of *Rg* group velocity show the SW region of the test site is characterized by faster velocities than the NE section. As an example, *Rg* with a period of 1 sec propagates with velocities greater than 2.3 km/sec for the SW section of the test site, while propagating at less than 2.3 km/sec for the NE section. Surface geologic maps and borehole lithology logs for the region show the slow region in the NE section of the test correlates well with sedimentary rocks and tuffaceous deposits overlain by alluvium. A large granodiorite body that has intruded the sedimentary rocks appears to correlate well with the fast velocities in the SW region. The inversions of the *Rg* dispersion curves give shear wave velocities for the SW region that are on average 0.4 km/sec greater than the NE region. At depths greater than 1.5 km the standard deviations for the models begin to overlap, and the statistical difference between the models is no longer significant.

The systematic variation in the relative patterns of *P* wave complexity and *P* and *Lg* source size estimators across the test site (Marshall *et al.,* 1985; Stewart, 1988; Ringdal *et al.,* 1992) correlate with the two geophysically distinct regions obtained from this study. Future studies should focus on the quantification of how the velocity structure at the test site influences the regional and teleseismic nature of *P* and *Lg* wave seismograms.

ACKNOWLEDGEMENTS

The authors wish to thank Brian Stump, Bob Herrmann, and Howard Patton for insightful suggestions concerning the research. We also wish to thank Diane Baker and Los Alamos National Laboratory for providing the raw and instrument corrected data along with details concerning the explosions at the test site. We wish to thank Luke Kluchko of DSWA for his support and expertise. Much of the information about the 1998 borehole closures including borehole lithology and rock properties was provided by the Institute of Geophysical Research of the National Nuclear Center of the Republic of Kazakhstan (NNC), and we wish to thank them for their help with this experiment. The research was sponsored by the Office of Nonproliferation and National Security and the Office of Research and Development for the Department of Energy under contract no. W-7405-ENG-26.

REFERENCES

Bache, T.C., S.R. Bratt, and H. Bungum, (1986). High-frequency P-wave attenuation along five teleseismic paths from central Asia, Geophys. *J. R. astr. Soc*., 85, 505-522.

Borovikov, L.E., 1972, Tectonic map of central and eastern Kazakhstan, scale 1:1000000, Sheet 2.

Davis, P.A., and G.L. Berlin (1992). Geologic mapping of the Semipalatinsk region, eastern Kazakhstan, using land sat thematic mapper and spot panchromatic data, Los Alamos National Laboratory, LAUR-92-310, 15p.

Dziewonski, A., S. Bloch and M. Landisman (1969). A technique for the analysis of transient seismic signals, *Bull. Seism. Soc. Am.* 59, 427-444.

Glenn, L., and S. Myers (1997). Depth of burial experiment at Balapan, Lawrence Livermore National Laboratory, UCRL-JC-128313.

Gupta, I.N., W.W. Chan, and R.A. Wagner (1992). A comparison of regional phases from underground nuclear explosions at East Kazakh and Nevada Test Sites, *Bull. Seism. Soc. Am.* 82, 352-382.

Herrin, E. and T. Goforth (1977). Phase-matched filters: application to the study of Rayleigh waves, *Bull. Seism. Soc. Am.* 67, 1259-1275.

Herrmann, R.B. (1988). *Computer Programs in Seismology.* Vols II-IV, St. Louis University, St. Louis, Missouri.

Jih, R.S., and R.A. Wagner, (1992). Path-corrected body-wave magnitudes and yield estimates of Semipalatinsk explosions, Teledyne-Geotech, TGAL-92-05, Alexandria, Virg., 69pp.

Kocaoglu, A. and L.T. Long (1993). Tomographic inversion of *Rg* wave group velocities for regional near-surface structure, *J. Geophys. Res.* 98, 6579-6587.

Leith, W. (1987). Tectonics of eastern Kazakhstan and implications for seismic source studies in the Shagan River area, in Paper Presented at the 9th annual DARPA/AFGL Seismic Research Symposium, 15-18 June 1987, pp. 34-37.

Marshall, P.D., T. C. Bache, and R. C. Lilwall (1985). Body wave magnitudes and locations of Soviet underground explosions at the Semilpalatinsk test site, AWRE Report No. 0 16/84 (re-issue), HMSO, 87.

Mayeda, K. and W. Walter (1996). Moment, energy, stress drop, and source spectra of western United States earthquakes from regional code envelopes, *J. Geophys. Res.* 101, 11195-11208.

Meyers, S.C., W. R. Walter, K. Mayeda, and L. Glenn (1999). Observation in support of *Rg* scattering as a source of explosion S waves: regional and local recordings of the 1997 Kazakhstan depth of burial experiment, *Bull. Seism. Soc. Am*. 89, 544-549.

Mueller, R.A., and J.R. Murphy (1971). Seismic characteristics of underground nuclear detonations, *Bull. Seism. Soc. Am*., 61, 1675-1692.

Nalivkin, D,V. (1960). The geology of the USSR. A short outline (including a 1:7,500,000 scale geologic map), Pergammon Press, New York, 170p.

NNC Field Report (1996). Unused vertical borholes at the Balapan test field of the former Semipalatinsk test site; review of existing data on the boreholes geology and design, National Nuclear Center of the Republic of Kazakhstan, Kurchatov city, Republic of Kazakstan.

Patton, H.J., and S. R. Taylor (1995). Analysis of *Lg* spectral ratios from NTS explosions: implications for the source mechanisms of spall and the generation of *Lg* waves, *Bull. Seism. Soc. Am.* 85, 220-236.

Phillips, W.S., H. E. Hartse, S. R. Taylor, A. A. Velasco, and G. E. Randall (1999). Regional phase amplitude tomography for seismic verification, PAGEOPH, submitted.

Ringdal, F., P. D. Marshall, and R. W. Alewine (1992). Seismic yield determination of Soviet underground nuclear explosions at the Shagan River test site, *Geophys. J. Int.* 109, 65-77.

Stewart, R.C., (1988). P-wave seismograms from underground explosions at the Shagan River Test Site recorded at four arrays, AWE Report O 4/88, Aldermaston, UK, 249pp.

Thurber, C.H., H. R. Quin, and R. Saleh (1994). Catalog of Locations of Nuclear Explosions at Balapan, Kazakhstan, 1965 to 1985, *Bull. Seism. Soc. Am.,* 84, 458-461.

Zonenshain, L.P., M.I. Kuzmin, and L.M. Natapov (1990). Geology of the USSR: a plate-tectonic synthesis, B.M. Page, Ed., American Geophysical Union Geodynamic Series, 21, 242p.

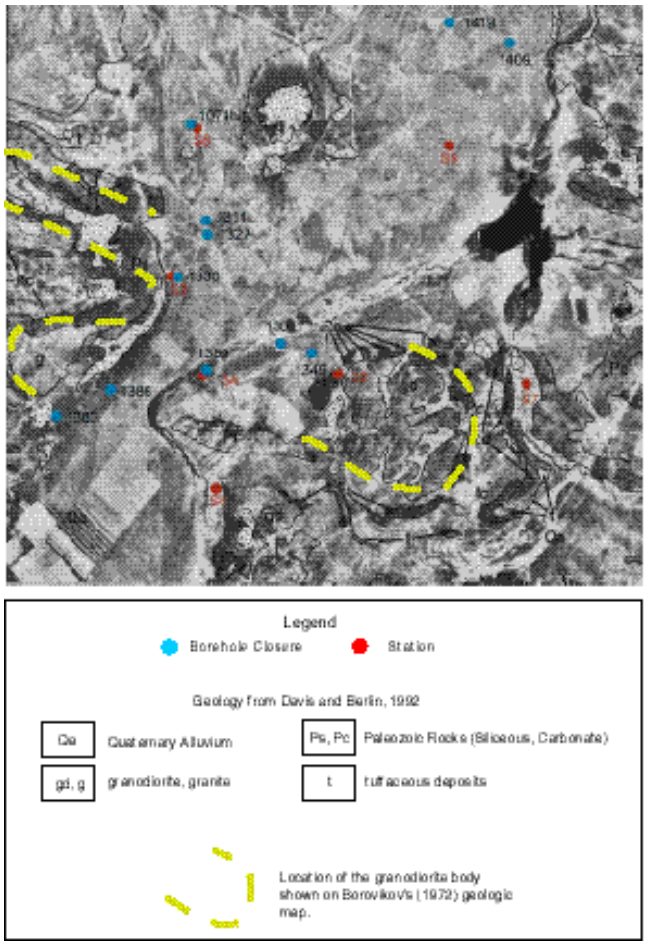

Figure 1. Land Sat image of the STS with superposed geologic units (modified from Davis and Berlin, 1992). The locations of the boreholes and seismic stations for this study are also shown. The approximate outline of the granodiorite body shown on Borovikov's (1972) regional scale geologic map is also shown. The granodiorite body (or similar lithology) is mapped in both 1311 and 1327 boreholes.

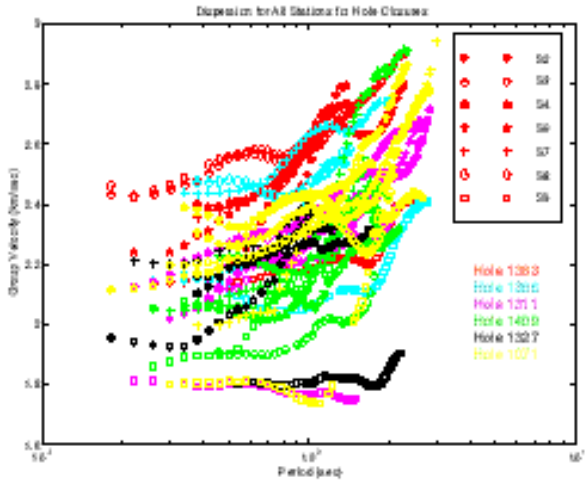

Figure 2. *Rg* group velocity dispersion curves for all station-event pairs processed in this study.

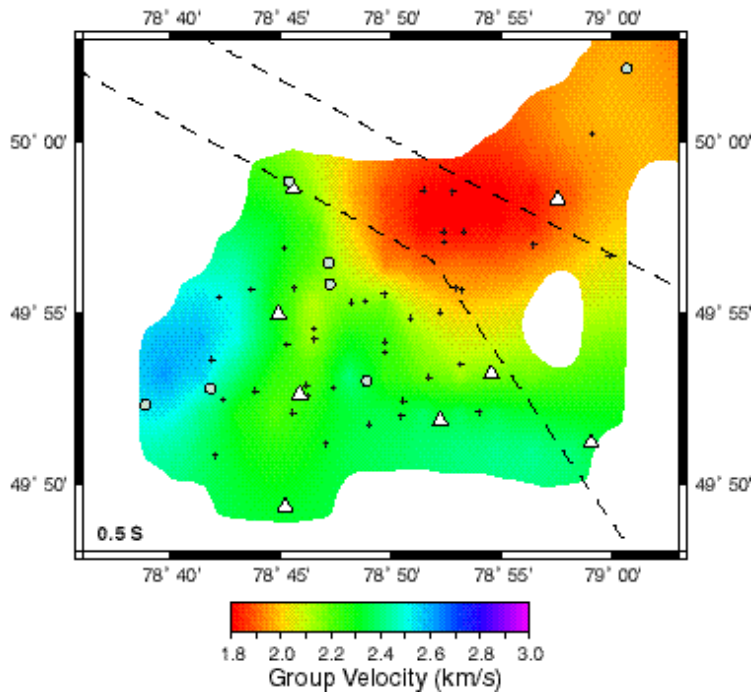

Figure 3. Tomographic map of *Rg* velocities at T=0.5 sec. The stations and explosions are shown by triangles and circles respectively, while the midpoints for each path are shown as plusses. The dashed lines show the subregions of the STS as determined by magnitude residuals (m_b-m_{Lg}) from Ringdal *et al.* (1992).

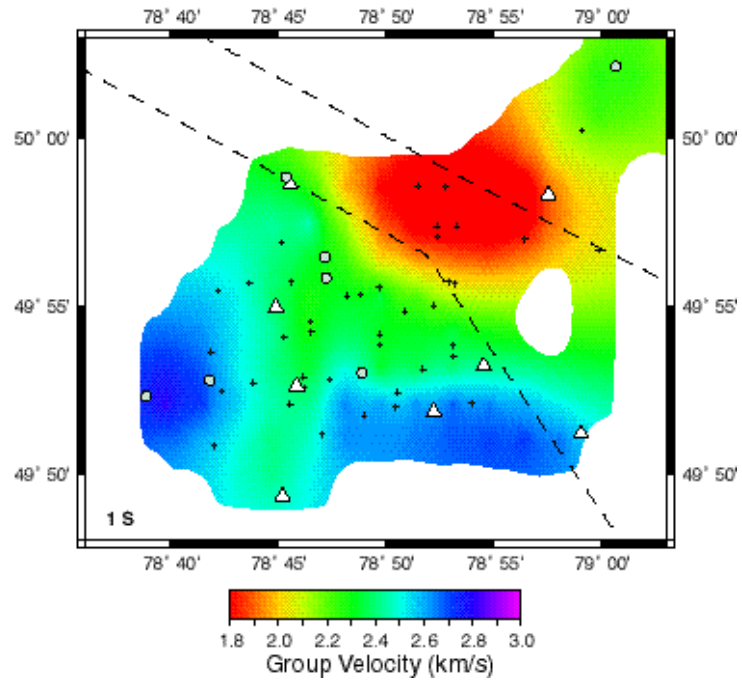

Figure 4. Tomographic map of *Rg* velocities at T=1 sec.

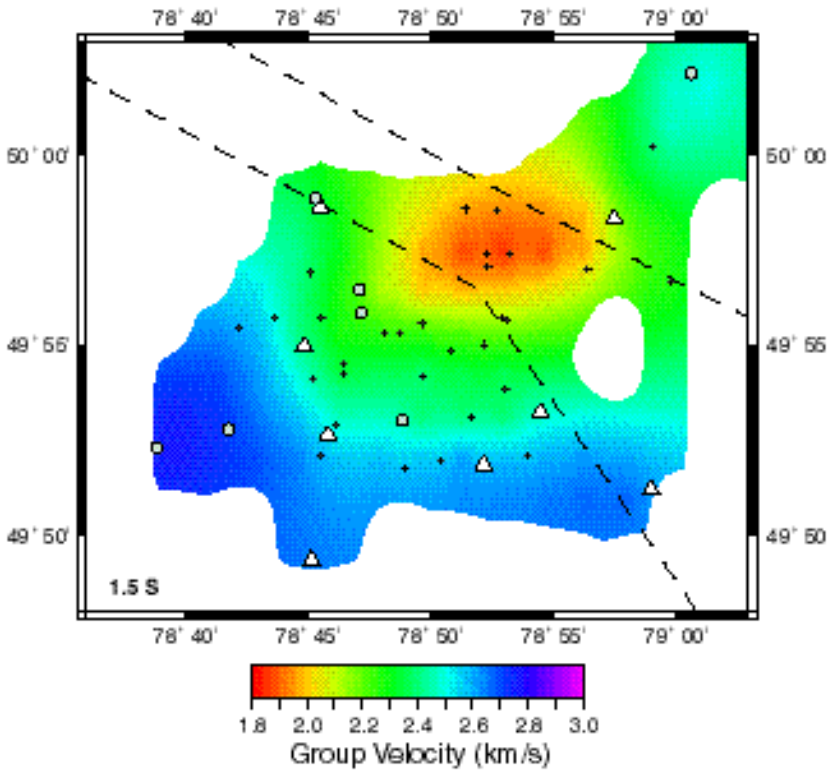

Figure 5. Tomographic map of *Rg* velocities at T=1.5 sec.

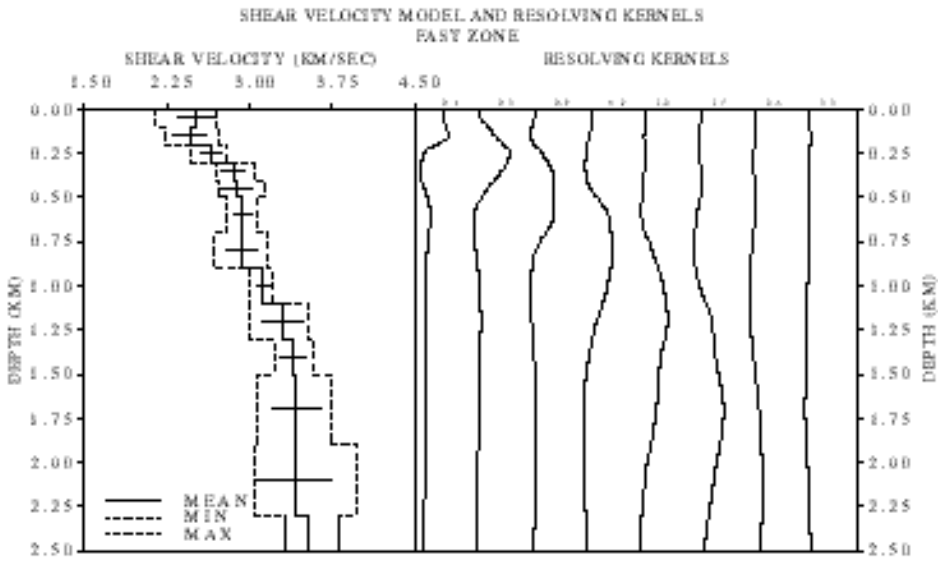

Figure 6. Inversion for shallow shear wave velocity structure in the SW region of the STS. The range of all velocity models that fit the observed dispersion are shown by the dashed lines, and the solid line shows the average velocity structure. The final velocity models show little deviation from the starting model at depths greater than 2.5 km because of loss of resolution as noted in the normalized resolution kernels.

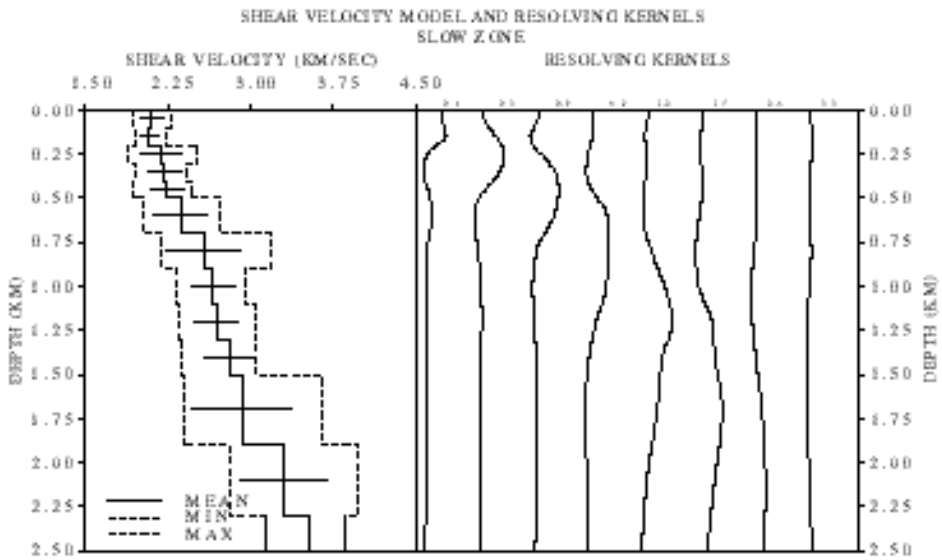

Figure 7. Dispersion results for the inversion of the 1383 to S7 dispersion curve. The observed data is shown as circles with error bars, while the theoretical dispersion from the inversion is shown as the line.

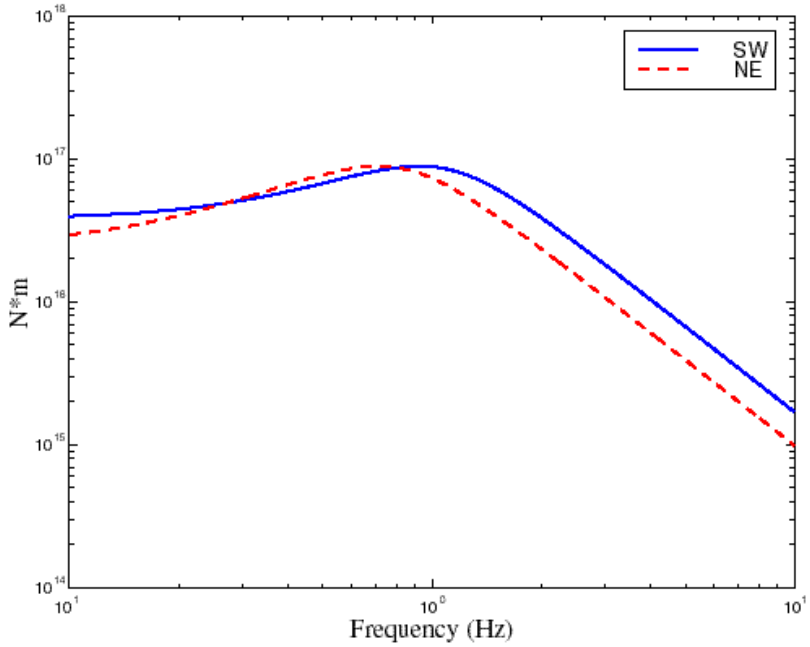

Figure 8. Reduced Velocity Potential (RVP) spectra for two identical explosions in geologic structures representative of the NE and SW regions of STS.